AIAA Aviation
16-20 June 2014, Atlanta, GA
20th AIAA/CEAS Aeroacoustics Conference

Trailing edge noise of partially porous airfoils

Thomas Geyer* and Ennes Sarradj†
Brandenburg University of Technology Cottbus - Senftenberg, 03046 Cottbus, Germany

The use of porous trailing edges is one possible approach to reduce airfoil trailing edge noise. Past experiments on fully porous airfoil models showed that a noticeable noise reduction can be achieved. However, this reduction is accompanied by a loss in aerodynamic performance. To combine the acoustic advantages of the porous trailing edge with the aerodynamic advantages of a non-porous airfoil, the generation of trailing edge noise of airfoil models that only have a porous trailing edge is investigated. To this end, initial experiments were performed on a set of airfoils with porous trailing edges of varying chordwise extent in an open jet wind tunnel, using microphone array measurement technique and a deconvolution beamforming algorithm. The lift forces and drag forces were measured simultaneously to the acoustic measurements. Additionally, hot-wire measurements were performed to allow conclusions on the underlying mechanisms that enable the noise reduction. It could be demonstrated that, depending on the porous material, airfoils that are non-porous except for their trailing edge can still lead to a noticeable trailing edge noise reduction, while providing a better aerodynamic performance.

List of symbols

c	[m/s]	sound velocity
c_l	[m]	chord length
f_c	[Hz]	center frequency
F_D	[N]	drag force
F_L	[N]	lift force
F_0	[N]	force used for normalization, $F_0 = 1$ N
Ma	[-]	Mach number
r	[Pa s/m^2]	air flow resistivity
L_p	[dB]	sound pressure level
Re	[-]	chord based Reynolds number
s	[m]	chordwise extent of porous material
Sr	[-]	chord based Strouhal number
Tu	[-]	turbulence intensity
u	[m/s]	turbulent velocity fluctuations
U	[m/s]	mean (time-averaged) flow velocity
U_0	[m/s]	free stream velocity (flow speed)
x	[m]	streamwise cartesian coordinate
y	[m]	spanwise cartesian coordinate
z	[m]	vertical cartesian coordinate
α	[°]	geometric angle of attack
Φ	[m^{2}s^{-1}]	third octave band turbulence spectra
Φ_0	[m^{2}s^{-1}]	used for normalization, $\Phi_0 = 1$ m^{2}s^{-1}
σ	[-]	volume porosity
τ	[-]	tortuosity

*Research Assistant, Chair of Technical Acoustics, Brandenburg University of Technology Cottbus - Senftenberg.
†Professor, Chair of Technical Acoustics, Brandenburg University of Technology Cottbus - Senftenberg.

I. Introduction

When a wing or an airfoil are subject to a fluid flow, a boundary layer develops along their surface on both suction side and pressure side. Depending on the flow speed and the dimensions of the wing, this initially laminar boundary layer may become turbulent, which means it contains unsteady vortices on many scales, called eddies. When these turbulent structures are convected over the trailing edge of the wing, broad band noise is generated.

Different approaches exist to reduce this generation of trailing edge noise from high lift devices and wings of fans, propellers or wind turbines. Such approaches include for example trailing edge serrations,[14,21,24] slitted trailing edges and brush-like edge extensions[9,15] or trailing edges made of metal mesh sheets.[16] Another means to reduce trailing edge noise is the use of porous materials. Chanaud et al.[5,6] examined the noise reduction of propeller fans that were composed of porous blades. They successively closed the pores of the blades with increasing fan diameter and obtained a noticeable noise reduction until only the outer 12.5 % of the blades (relative to the fan diameter) were left porous. Bohn[2] investigated the noise generation from a flat plate that was equipped with porous trailing edge extensions of varying streamwise extent. He found a maximum noise reduction at a frequency proportional to the ratio of flow speed to the streamwise extent of the porous material. Revell et al.[25] measured the noise generated by trailing-edge flaps whose side edges were treated with porous materials and observed a noise reduction over a large range of frequencies. Revell et al. even took into account the dependence of the material's air flow resistance on the flow speed. More recent experiments by Geyer et al.[10,12] on airfoils made completely out of porous materials also confirmed their noticeable noise reduction potential. After a first attempt to establish a noise prediction model based on spectra of the turbulent velocity fluctuations measured in the boundary layer of the porous airfoils,[12] the large amount of measurement data was then used to build symbolic regression models for the noise generation by porous airfoils.[29] The resulting trailing edge noise models showed a general dependency of the sound power on the fifth power of the flow velocity. The frequency spectrum of the noise was found to be governed by the flow resistivity of the porous materials. However, the noise reduction observed in the experimental studies was connected to a loss in aerodynamic efficiency, meaning a reduced lift and an increased drag compared to a non-porous airfoil with identical shape and dimensions. Additional hot-wire measurements by Geyer et al. on a subset of the porous airfoils showed the influence of the porous consistency on the turbulent boundary layer.[11,12] Jaworski and Peake[18] analytically studied the effect of poroelastic trailing edges, combining the effect of elasticity and porosity, on the reduction of airfoil trailing edge noise. They found that the porous consistency has an influence on the dependency of trailing edge noise on the flow speed: While the trailing edge noise of an impermeable rigid plate depends on the fifth power of the flow speed, which is in agreement with basic theory,[8] a highly permeable plate shows a dependency on the sixth power.

One conclusion from the basic study on porous airfoils by Geyer et al.[10] is the idea to perform experiments on partially porous airfoil models. Such airfoils are non-porous at the leading edge and over the greater part of the surface, but have a porous trailing edge. Thereby, the aim is to combine the aerodynamic advantages of a common non-porous airfoil (high lift, low drag) with the acoustic advantages of a porous airfoil (low trailing edge noise generation). Besides the use of such partially porous airfoils, another possible approach to make up for the aerodynamic deficits of fully porous airfoils would be an increase in angle of attack. This, however, is accompanied by other aerodynamic and aeroacoustic disadvantages and is not subject of the present study.

Based on the results obtained by Geyer et al.[10,12] for fully porous airfoils and inspired by the work of Bohn,[2] the noise generation of airfoils with a varying chordwise extent of the porous material (partially porous airfoils) is examined in the present paper. The results of preliminary measurements using some of the porous airfoils from reference[10] will be presented.

The remainder of the paper is organized as follows: First, the experimental setup is described in detail, including the airfoil models, the wind tunnel, the setup used for the measurement of the aerodynamic forces, the microphone array technique as well as the corresponding data processing algorithms and the setup for the constant temperature anemometry measurements. Second, the results of the different experiments are presented and discussed. Finally, the findings of the present study are summarized.

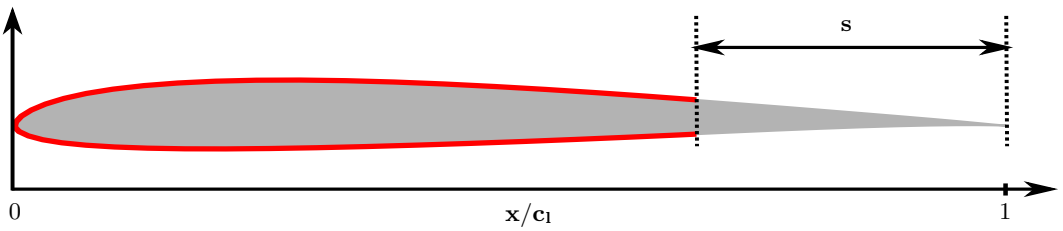

Figure 1. Schematic of a partially porous airfoil (gray: porous airfoil, red: flexible, impermeable foil used to cover the pores at the front part of the airfoil, s: chordwise extent of the porous material)

II. Materials and methods

The experimental setup used for the present study is generally similar to that used by Geyer et al.,[10] and therefore only a basic description will be given here. Experiments were performed on a set of airfoils with a varying extent of porous material in an open jet wind tunnel. A microphone array was used for the acoustic measurements, while simultaneously the aerodynamic performance of the airfoils was captured. Additional constant temperature anemometry measurements were performed above the trailing edge and in the wake of a subset of the airfoils.

II.A. Airfoil models

II.A.1. Porous materials

The porous materials used for the manufacturing of porous airfoils are mainly characterized in the present study by their air flow resistivity r, which is a measure for the resistivity of an open-porous material against a fluid flow through the material. It is believed to be the parameter that has the most influence on the noise reduction of the porous airfoils and is measured according to ISO 9053.[17] In addition it was found that the porous airfoils should also have a volume porosity σ which is not too low in order to allow for a noticeable trailing edge noise reduction.[12] This parameter describes the ratio of the volume of the pores to the total volume of the porous material. The acoustically most effective materials from[10,12] had porosities in the order of 0.9 and above. Another parameter that may be useful to describe the properties of the porous materials is their tortuosity τ, which is the squared ratio of the effective length of the flow path through the pores of the porous material to the minimum length between flow inlet and outlet.[7] It is hence a measure for the curvature or twistedness of the pores.

It can be assumed that the air flow resistivity r is mainly governed by two parameters, the size of the pores as well as the tortuosity, as an increase in pore size would obviously result in a decrease in air flow resistivity, while an increase in tortuosity would lead to an increasing air flow resistivity.

II.A.2. Airfoils

Due to the positive results regarding the noise reduction achieved by the porous airfoils used in the previous study[10] and due to the fact that these airfoils were already available, it was decided to use the same airfoils in the present study. In order to build the desired airfoils with different chordwise extents of porous material, basically two methods may be pursued: The first would be to fill the open pores of the porous materials except for the aft part of the airfoils, an approach also used by Chanaud et al.[5,6] This, of course, would most likely be a permanent measure and thus would prevent any future experiments on the original, fully porous airfoil models. This method may even require additional effort to even the surface of the then non-porous part of the airfoil. The second method, which was chosen for the present investigation, is to simply cover the desired part of the surface of the porous airfoils using a thin, impermeable foil. Figure 1 shows a schematic of the resulting partially porous airfoil.

Different films and tapes were examined regarding their usability for the intended experiments. The best adhesion on the porous surfaces could be achieved by a thin, flexible polyvinyl chloride (PVC) film. Due to the fact that it should be possible to completely remove the tape from the surface of the airfoils residue-free after the experiments (without clogging the pores or destroying the surface), only a small subset of the 16 porous airfoils used in the previous experimental study[10] could also be used for the present study.

Table 1. Materials used for the manufacturing of the airfoils (given is the air flow resistivity r, measured according to ISO 9053[17])

Name	Material	r [Pa s/m^2]
Reference	non-porous	∞
Porex	polyethylene granulate	316,500
Arpro Porous 4025	expanded polypropylene foam	23,100
Recemat	metal foam	8,200
M-Pore PU 45 ppi	polyurethane foam	1,500
M-Pore Al 45 ppi	metal foam	1,000

Practically, this meant a limitation to the rigid porous materials. The remaining airfoil models suitable for the present study are given in Table 1. By using the impermeable foil, airfoils with different chordwise extents s of the porous material were realized (see Figure 1). Normalized by the airfoil chord length, this extent took values of 0.05, 0.1, 0.2, 0.3, 0.5 and 1 (fully porous). However, not all extents were applied to each airfoil from Table 1.

Besides the porous and partially porous airfoils, measurements were also performed on a non-porous reference airfoil for reasons of comparison. All airfoils of the present study have an SD7003 shape with a chord length c_l of 235 mm and a span width of approximately 400 mm. Due to manufacturing reasons, the trailing edge thickness of the porous airfoils was increased to nominally 1.59 mm compared to 0.5 mm of the reference airfoil[10] (in practice, it is difficult to measure the thickness of the porous trailing edges exactly, especially for materials with very large pores). The reference airfoil as well as the partially porous airfoils were provided with thin tripping tape at 10 % of the chord on both suction side and pressure side to enforce the transition to a fully turbulent boundary layer. The tape that was used was *Anti-slip tape*, which has a coarse surface, with a height of approximately 0.8 mm and a width of 2 mm. No tripping tape was applied to the fully porous airfoils since their surface roughness ensured the existence of a turbulent boundary layer.[11]

II.B. Aeroacoustic wind tunnel

All measurements were performed in the small aeroacoustic wind tunnel at the Brandenburg University of Technology in Cottbus, an open jet wind tunnel which was equipped with a circular nozzle with a diameter of 0.2 m. At the time of the measurements, this setup allowed for maximum flow speeds of approximately 60 m/s. The turbulence intensity directly in front of this nozzle is in the order of 0.1 % at a flow speed of 20 m/s, characterizing the flow as virtually not turbulent. At a flow speed of 50 m/s, the A-weighted overall sound pressure level generated by the wind tunnel, measured at a distance of 1 m at an angle of 90° to the nozzle axis, is below 60 dB. Additional information on the wind tunnel can be found in the work by Sarradj et al.[26]

During the measurements, the airfoils were positioned at a distance of 0.05 m to the nozzle exit by lateral mountings that were themselves located outside of the flow to prevent any generation of unwanted aeroacoustic noise (see Figure 2(a)).

II.C. Measurement of the aerodynamic forces

To allow conclusions on the aerodynamic performance of the airfoils, both the lift force F_L and the drag force F_D were captured simultaneously to the acoustic measurements. As in the previous experiments on fully porous airfoils,[10] the aerodynamic measurements were performed using a six component balance that consists of six single point load cells, each of which has a nominal load of 10 kg. Load cells with such a relatively high nominal load were chosen since they have to bear not only the weight of the airfoils plus a (negative) lift force at angles of attack below zero, but also the weight of the heavy steel frame that holds the lateral mountings and the airfoil. The data from the six load cells were recorded with a sample frequency of 10 kHz and a measurement duration of 3 s using a National Instruments 24 Bit full bridge analog input module. Figure 2(a) shows a photograph of the measurement setup including the balance. Where possible, the balance was covered with absorbing foam to minimize acoustic reflections.

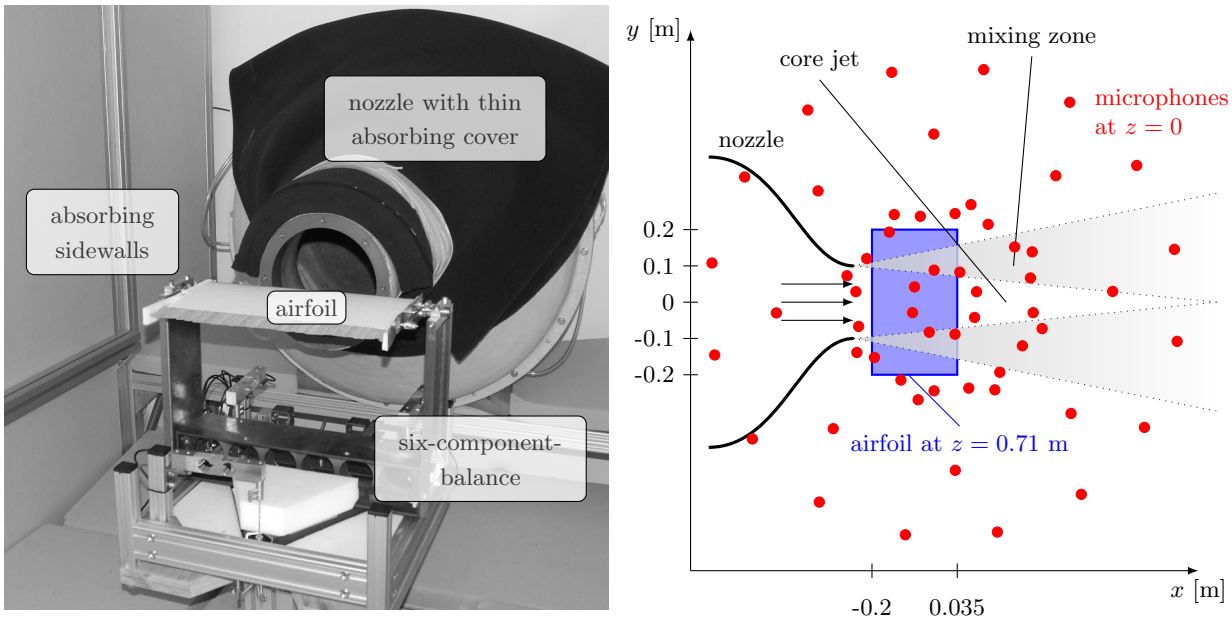

(a) Photograph including the partially porous airfoil made of M-Pore Al 45 ppi with $s/c_l = 0.1$

(b) Schematic (top view, flow from left to right)

Figure 2. Experimental setup in the aeroacoustic wind tunnel

The majority of measurements were performed at zero angle of attack. On a subset of the airfoils, measurements were performed at non-zero angles, but only for one flow speed. Common corrections for the angle of attack, like that proposed by Brooks et al.,[3] cannot be applied to the present setup due to the expanding jet width, the cambered airfoil shape and the porous consistency of the airfoils.[10] Therefore, the geometric angle of attack α is only given as a means of comparison between different working points of the airfoils.

II.D. Microphone array measurements and data processing

In this section, attention is paid to the microphone array measurement technique and, in particular, to the processing of the measured data using deconvolution beamforming algorithms.

II.D.1. Measurement setup and initial data processing

The measurements were performed using a planar microphone array that consists of a 1.5 m × 1.5 m aluminum plate and holds 56 flush-mounted 1/4th inch microphone capsules. It was positioned out of the flow, at a height of 0.71 m above the airfoils (Figure 2(b)). The raw acoustic data were recorded with a sample frequency of 51.2 kHz and a duration of 40 s (2,048,000 samples) using a National Instruments 24 Bit multichannel measurement system. This lead to a data amount of approximately 438 MBytes per measurement. The data were blockwise transformed into the frequency domain using a Fast Fourier Transformation (FFT) with a Hanning window on 50 % overlapping blocks with a size of 4,096 samples each. The resulting cross spectra of the 999 blocks were then averaged to obtain the cross spectral matrix. In a first step, the data were processed using a conventional delay and sum beamforming algorithm.[22]

II.D.2. Deconvolution beamforming

In a next step, deconvolution beamforming algorithms were applied to the data in order to remove the influence of the array point spread function on the results. Usually, the results of such algorithms are mapped onto a two-dimensional plane, as was done in the experiments presented in reference.[10] In the present case, in order to achieve a better depth resolution,[28] the results are calculated for and mapped onto a fully three-dimensional grid.

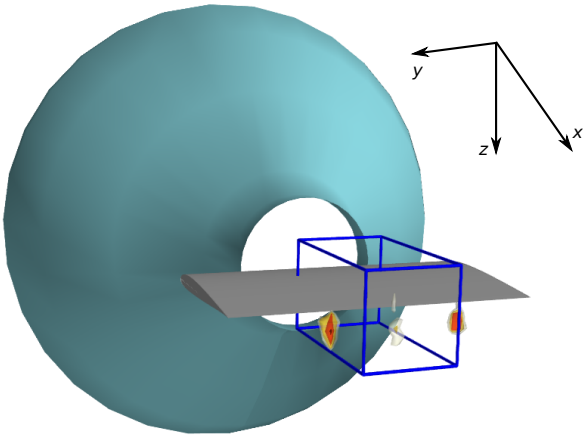

Figure 3. Three-dimensional volume used for the integration of the noise source contributions in order to obtain trailing edge noise spectra

For the analysis of airfoil trailing edge noise, different algorithms, such as DAMAS,[4] CLEAN-SC[30] and orthogonal beamforming,[27] are commonly used and known to produce good results. Since the orthogonal beamforming is computationally fast and was found in past studies to be well suited for the three-dimensional analysis of edge noise from porous airfoils,[12,13] it was decided to use this algorithm also for the analysis of the measurement data from partially porous airfoils.

In general, three noise sources are located at the trailing edge of the airfoils (see Figure 3): two strong lateral sources, which are caused by the interaction of the wind tunnel shear layer with the airfoil trailing edge, and the source of interest, generated by the interaction of the turbulent boundary layer with the trailing edge within the wind tunnel core jet. Interestingly, in case of the partially porous airfoils the sound maps showed that, depending on the air flow resistivity, the trailing edge sources may be located in the streamwise direction approximately near the aft end of the flexible foil, and hence at the position where the airfoil becomes porous.

In order to obtain sound pressure level spectra from the three-dimensional sound maps, an integration was performed over a three-dimensional source volume inside the map grid that only contains the noise sources generated by the interaction of the turbulent boundary layer with the airfoil trailing edge. Background noise source positions, like the wind tunnel nozzle, the airfoil leading edge and the positions of the two lateral sources generated by the wind tunnel shear layer interacting with the trailing edge, were excluded from the integration. A schematic of the resulting sector is shown in Figure 3. The spectra were then converted to third octave bands $re\ 2{\cdot}10^{-5}$ Pa.

Finally, to account for the reflection of sound at the rigid microphone array, 6 dB were subtracted from the resulting third octave band sound pressure levels (when comparing the present results with those obtained for the fully porous airfoils,[10] it has to be kept in mind that the 6 dB were not subtracted from the latter, as they were presented as measured).

II.E. Constant temperature anemometry measurements

In order to examine the influence of the porous trailing edges on the turbulence in the boundary layer, constant temperature anemometry measurements were performed on a subset of the airfoils using a Dantec single-wire boundary layer probe, with the wire aligned with the spanwise direction. The probe was positioned using a three-dimensional traverse system with a minimum step size of 0.1 mm. The data were recorded using a Dantec multichannel CTA measurement system with a sample frequency of 25.6 kHz and a measurement duration of 10 s. To avoid the possible influence of vibrations of the traverse after each step, the first two seconds were removed from each data set, leaving 204,800 samples to be analyzed. The CTA system contains an internal low pass filter with a cutoff frequency of 10 kHz.

Hot-wire measurements were conducted at several points along a vertical line at four chordwise locations: directly above the trailing edge of the airfoils and at three locations in the wake of the airfoil, at a distance of 5 mm, 10 mm and 20 mm from the edge, respectively. This adds up to about 330 measurement locations for each airfoil and each flow speed. The data were used to determine the turbulence intensity and the

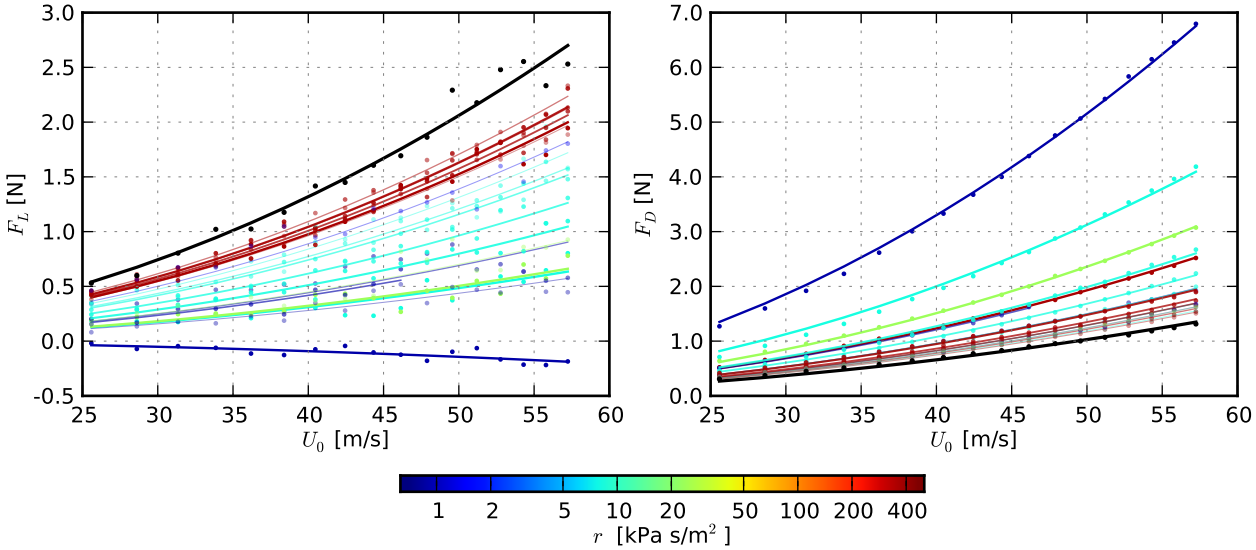

Figure 4. Lift force F_L and drag force F_D of all examined airfoils as a function of the flow speed U_0 at zero angle of attack (dots: measurement, lines: linear least squares fit according to $F \propto U_0^2$), the line width and the opacity of the lines increase with increasing extent of the porous materials

mean velocity profiles. Additionally, at single measurement positions the third octave band spectra of the turbulent velocity fluctuations Φ was calculated. To this end, the data were Fast Fourier transformed in blocks of 4,096 samples and averaged with an overlap of 50 %. A high pass filter with a cutoff frequency of 10 Hz was implemented into the analysis software to eliminate low frequency fluctuations generated by the wind tunnel.

III. Results

Acoustic measurements were conducted at zero angle of attack at 17 subsonic flow speeds U_0 between approximately 25 m/s and 57 m/s, corresponding to Mach numbers $Ma = U_0/c$ between 0.07 and 0.17 and chord based Reynolds numbers Re between $3.8{\cdot}10^5$ and $8.5{\cdot}10^5$. As mentioned above, a number of additional measurements were performed at non-zero angles of attack for only the maximum flow speed.

III.A. Aerodynamic forces

In a first step, the results from the aerodynamic measurements on the airfoils are presented since they are subsequently used for the scaling of the acoustic results. Figure 4 shows the measured lift and drag forces as a function of the flow speed. Additionally, the figures contain a least squares fit according to $F \propto U_0^2$ that can be expected according to basic aerodynamic theory. In general, two basic trends can be observed: First, as one would suspect, the lift force F_L increases with increasing air flow resistivity r and with decreasing extent s of the porous materials. Hence, the highest lift force is generated by the non-porous airfoil and by the porous airfoils made of the material with the highest air flow resistivity, Porex (r = 316,500 Pa s/m^2). Second, the drag force increases with decreasing air flow resistivity and increasing extent of the porous material. This is due to the fact that a lower air flow resistivity is, in the present case, accompanied by a higher surface roughness due to larger pores,[12] which leads to the increase in drag.

For some airfoils, a noticeable deviation of the measured lift forces from the theoretical fit can be seen from Figure 4. These deviations are measurement inaccuracies, most likely due to the relatively small lift forces that are measured at zero angle of attack, especially for porous airfoils with low air flow resistivities and a large extent of the porous material, compared to the high nominal load of the load cells. Although the number of samples of the aeroacoustic measurements has been increased compared to the measurements presented in,[12] it is still assumed that a larger number of samples, and hence a longer measurement duration, would result in a better agreement between measurement and theoretic fit. The deviation of the measured drag forces from the fit is much smaller.

For a smaller set of airfoils, additional measurements were performed at non-zero angles of attack for only

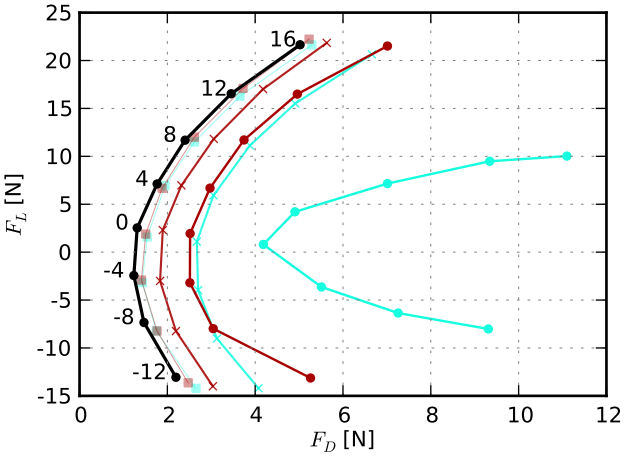

Figure 5. Polar plots of lift and drag forces of a subset of the airfoils at varying angles of attack α at $U_0 \approx 57$ m/s ($Ma \approx 0.17$); Recemat, $r = 8{,}200$ Pa s/m^2, $s/c_l =$ ■ 0.05, × 0.5, ● 1; Porex, $r = 316{,}500$ Pa s/m^2, $s/c_l =$ ■ 0.05, × 0.5, ● 1; ● non-porous reference airfoil, $r = \infty$ (numbers indicate geometric angle of attack)

the maximum flow speed. Figure 5 shows the resulting Lilienthal-type polar diagrams. It is again visible that a decrease in air flow resistivity r and an increase of the porous extent s lead to a decreasing lift, but an increasing drag. It can also be seen that, as would be expected, the semi-symmetric SD7003 airfoils generate a positive lift at zero angle of attack. The angle of attack at which no lift is generated is approximately between 0° and −4°.

III.B. Acoustic results

This section focuses on the presentation of the results from the acoustic measurements at zero angle of attack. Different scaling approaches are discussed.

Figure 6 shows the third octave band sound pressure levels of the trailing edge noise, calculated using the orthogonal beamforming as described in Section II.D, as a function of the chord based Strouhal number. The diagrams are arranged according to the extent s of the porous material, from $s/c_l = 0.05$ to $s/c_l = 1$. Thus, the last diagram of Figure 6 shows the trailing edge noise levels of the fully porous airfoils and is therefore similar to the results from the past studies by Geyer et al.[10,12] The sound pressure levels are scaled using the fifth power of the flow speed U_0, which is in accordance to basic aeroacoustic theory.[8] Although for porous trailing edges an exponent for the velocity dependence between 5 and 6 leads to better results,[29] the same exponent is used for all airfoils in order to enable a better comparison of the results.

Similarly, Figure 7 shows the scaled third octave band sound pressure levels of all airfoils as a function of the chord based Strouhal number. A presentation of the third octave band sound pressure levels as a function of a Strouhal number based on the chordwise extent of the porous materials, $f_c \cdot s/U_0$, as proposed by Bohn,[2] did not lead to a better collapse of the data.

The measured spectra of some of the porous airfoils show a narrow spectral peak. For the porous airfoil made of Porex ($r = 316{,}500$ Pa s/m^2) this peak is at a Strouhal number of approximately 10 to 12, independent of the extent of the porous material. The width of the spectral peak, however, seems to increase slightly with increasing porous extent. For the porous airfoils made of Recemat ($r = 8{,}200$ Pa s/m^2) and M-Pore Al 45 ppi ($r = 1{,}000$ Pa s/m^2), the peak Strouhal number decreases with increasing extent of the porous material, while the width also increases. This different behavior makes it difficult to interpret the cause of this peak. In case of the Porex airfoil, the trailing edge thickness of the airfoil may be responsible, where the differences in width of the spectral peak are caused by different turbulent boundary layer thicknesses due to the varying porous extent. Hence, the peak in this case may be a contribution of trailing edge bluntness noise. For the other airfoils, it can be assumed that the peak is also a contribution of trailing edge bluntness noise, but not due to the interaction of the boundary layer with the real trailing edge of the airfoil at $x = c_l$, but with the blunt edge at the aft end of the impermeable foil at $x = c_l - s$. The thickness of this "false edge" does indeed depend on the extent of the porous material. This assumption seems plausible taking into account the very high air flow resistivity of Porex (where the existence of a "false edge" would not be expected) compared to the low air flow resistivities of Recemat and M-Pore. At high Strouhal numbers,

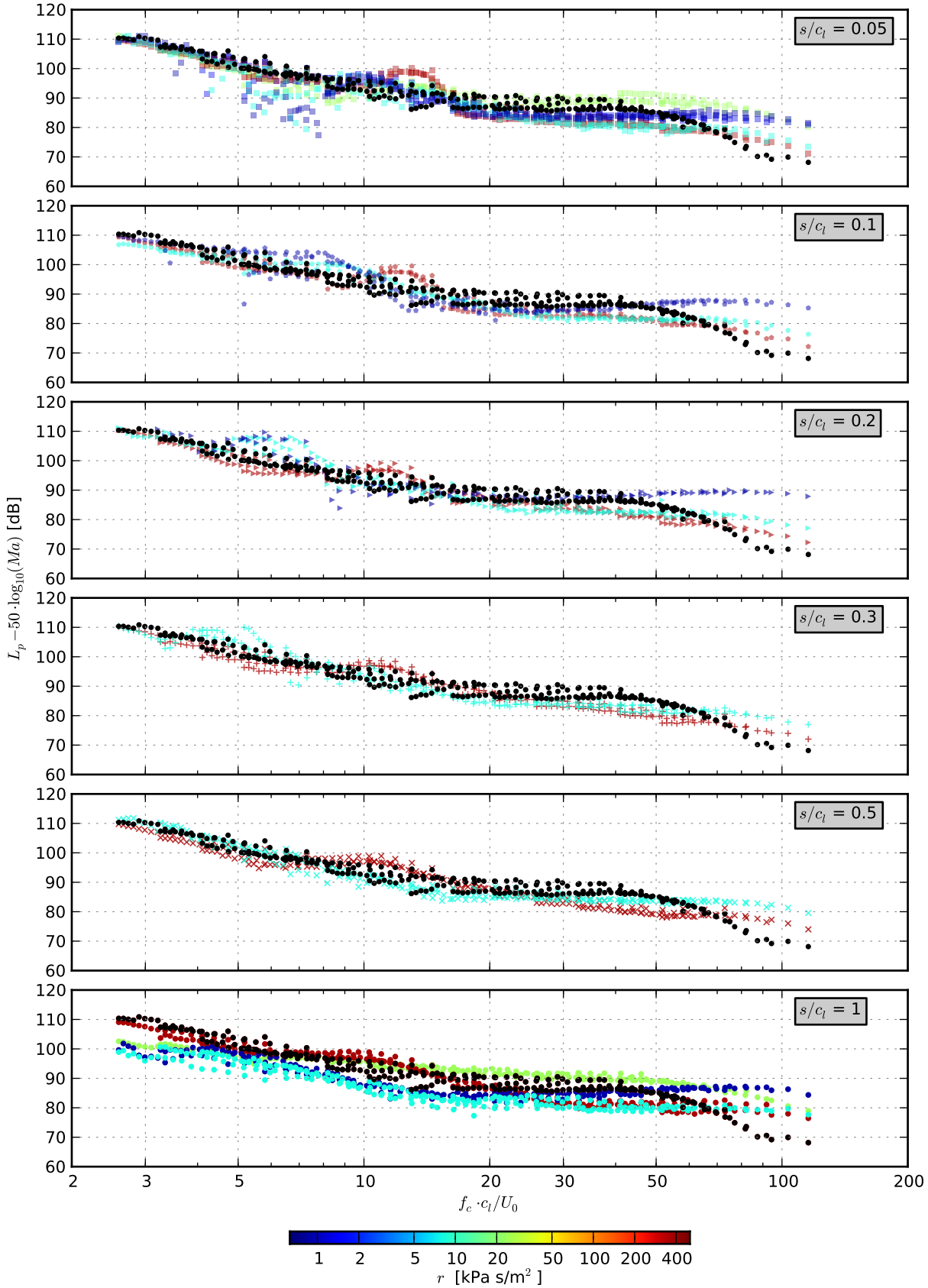

Figure 6. Trailing edge noise level of airfoils with different extents of the porous material, scaled with U_0^5, as a function of the chord based Strouhal number (black dots: non-porous reference airfoil), angle of attack $\alpha = 0^\circ$

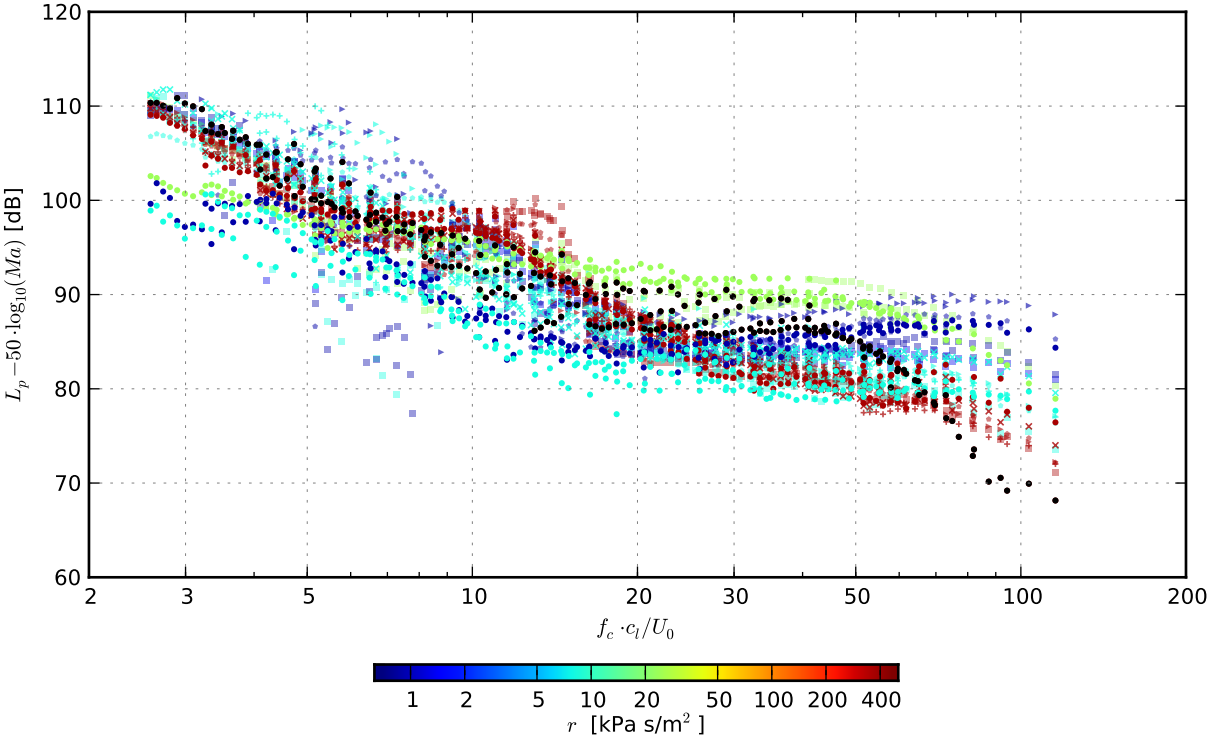

Figure 7. Trailing edge noise level of all examined airfoils, scaled with U_0^5, as a function of the chord based Strouhal number (black dots: non-porous reference airfoil), angle of attack $\alpha = 0^\circ$

porous airfoils tend to generate more noise than the reference case, which is assumed to be a contribution of surface roughness noise at high frequencies.[11]

It can be concluded from Figure 6 that, judging strictly by their noise reduction ability without consideration of aerodynamic performance, the fully porous airfoils perform best. A noise reduction in the order of 10 dB is possible (for example for the airfoil made of Recemat, $r = 8{,}200$ Pa s/m^2). This noise reduction was measured in a Strouhal number range approximately between 10 and 70. An increase of the porous extent s leads to a decrease of the trailing edge noise radiated into the far field. Still, even when the porous extent is only 5 % of the chord (uppermost diagram in Figure 6), the use of porous materials enables a noise reduction at medium Strouhal numbers, approximately between 20 and 50. Hence, even the use of porous trailing edges with such a small streamwise extent results in a noticeable broadband noise reduction.

Judging by their material properties, Figure 6 reveals that porous airfoils with medium to high air flow resistivities are favourable for a high trailing edge noise reduction, as for example the airfoils made of Porex ($r = 316{,}500$ Pa s/m^2) or Recemat ($r = 8{,}200$ Pa s/m^2). This is in accordance to the findings from the past experiments on fully porous airfoils.[10,12]

To include the aerodynamic performance of the airfoils into the analysis, different approaches were tested that make use of the measured aerodynamic forces. In a relatively simple approach, the measured lift force F_L is directly used for the scaling of the trailing edge noise, a method also employed by Lasagna et al. for the scaling of airframe noise[19] and by Lilley in his study of the silent flight of owls.[20] The resulting third octave band sound pressure levels, which can be interpreted as the noise generated per unit lift force, are presented in Figure 8. Note that, as the lift force is assumed to depend on the square of the flow speed U_0, the remaining Mach number dependence is reduced to a $(Ma)^3$ dependence.

When comparing the data from Figure 8 with the results from Figure 6 it is now visible that some porous airfoils do not lead to a noise reduction at all due to their relatively poor aerodynamic performance. Additionally, the frequency range at which a noise reduction may be obtained by other porous airfoils is now smaller. The porous materials that, under consideration of aerodynamic performance, are less feasible are of course those with low air flow resistivities, since a low air flow resistivity leads to a considerably lower lift generation compared to the non-porous reference airfoil (see Section III.A). One porous airfoil for which this effect can be observed very clearly is the airfoil made of M-Pore Al 45 ppi ($r = 1{,}000$ Pa s/m^2). For

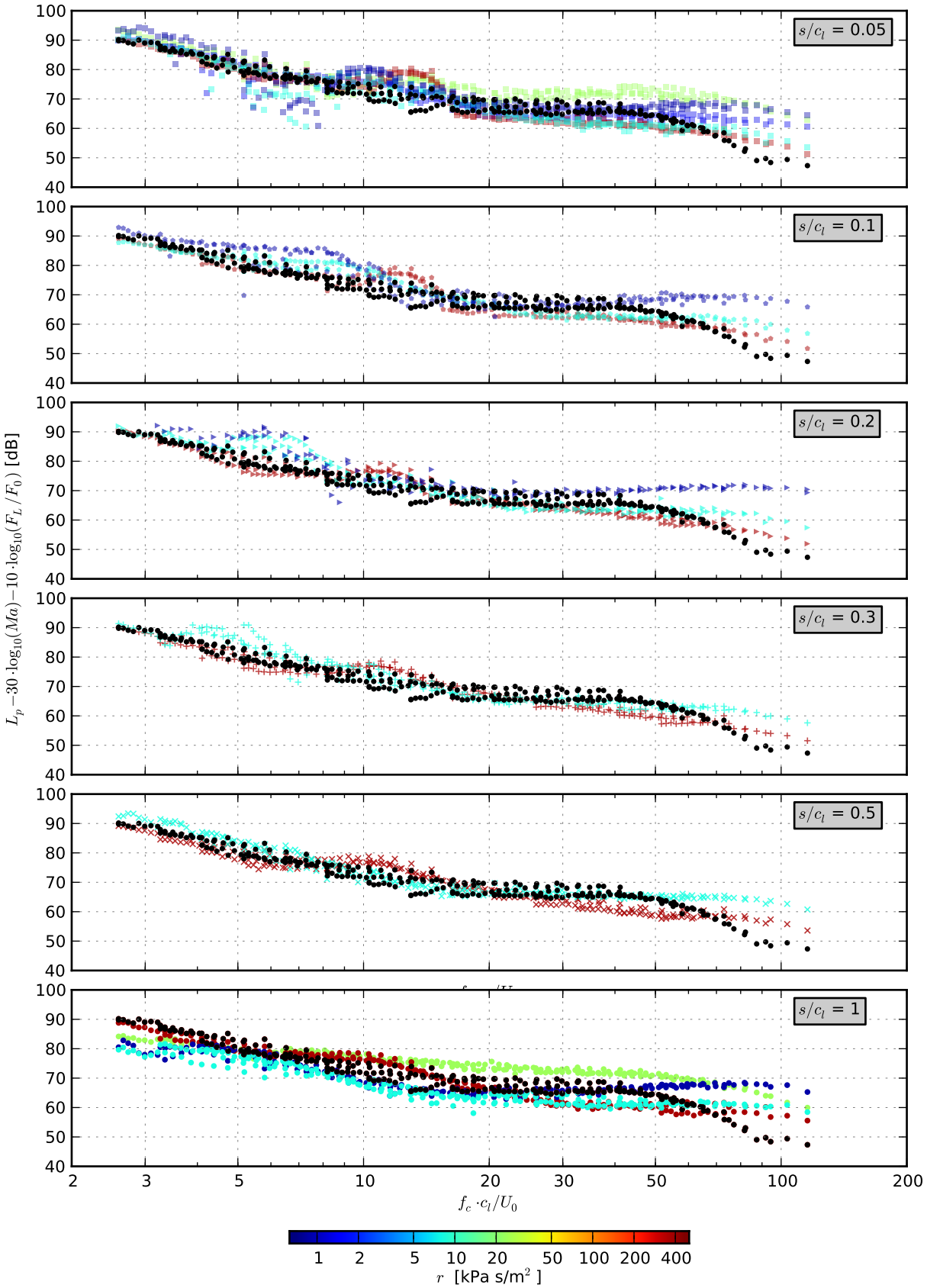

Figure 8. Trailing edge noise level of airfoils with different extents of the porous material, scaled with U_0^3 and the measured lift force F_L, as a function of the chord based Strouhal number (black dots: non-porous reference airfoil), angle of attack $\alpha = 0^\circ$

example, for $s/c_l = 0.05$ the porous trailing edge made of M-Pore Al 45 ppi clearly leads to a noise reduction for Strouhal numbers approximately between 15 to 50 without consideration of aerodynamic performance (Figure 6), while its trailing edge noise is similar to that of the non-porous reference airfoil when scaled with F_L (Figure 8).

However, Figure 8 shows that porous airfoils with high air flow resistivities, as for example the airfoil made of Porex (r = 316,500 Pa s/m^2), are still feasible in a Strouhal number range from approximately 20 to 70, even with only a small streamwise extent of the porous material.

To examine the influence of the porous extent in more detail, Figure 9 shows the scaled trailing edge noise spectra at only one flow speed as a function of frequency measured for three porous airfoils and the non-porous reference airfoil. Potential trends regarding the influence of the porous extent s on the noise reduction are now better assessable than from Figure 8. In general, it is visible that a trailing edge noise reduction is only obtained in a range of high frequencies between approximately 4 kHz and 10 kHz for the two airfoils with the higher air flow resistivities, Porex and Recemat (r = 316,500 Pa s/m^2 and r = 8,200 Pa s/m^2, respectively). At lower frequencies the sound pressure levels of both airfoils, when scaled with the measured lift force, exceed that of the reference airfoil. This is especially true for the airfoil made of Recemat, since the frequency range in which this particular airfoil generates more noise than the reference airfoil is much wider than for the airfoil made of Porex. The airfoil with the lower air flow resistivity, M-Pore Al 45 ppi (r = 1,000 Pa s/m^2) does not lead to a noise reduction (except in two cases in a small frequency range around 1.25 kHz and 1.6 kHz that are insignificant compared to the increased trailing edge noise generation at other frequencies). At very high frequencies, the noise generated by the airfoils with lower air flow resistivities (Recemat and M-Pore Al 45 ppi) exceeds the noise from the reference airfoil, which is supposedly due to the contribution of surface roughness noise.

Regarding the porous extent s that results in the lowest trailing edge noise reduction, Figure 9 shows that the influence of s is not very clear, since the difference in noise reduction in the frequency range between 4 and 10 kHz is in the order of about 2 to 4 dB only. Still, the results indicate that a larger porous extent is still favourable, at least for the airfoil made of Porex (r = 316,500 Pa s/m^2), which is supposed to be due to the high air flow resistivity and the resulting high lift force. This causes only minor differences in the scaling as opposed to porous airfoils with low air flow resistivities. For the airfoil made of Recemat, a large extent of the porous material also leads to good results regarding the noise reduction in this frequency range. Additionally, however, an extent of only 5% of the chord also leads to comparatively good results. This is assumed to be due to the better aerodynamic performance of the airfoil with this extent, leading to a lower sound pressure level when scaled with the lift force.

It can be concluded that the choice of the porous material seems to have a greater influence on the trailing edge noise spectra, when scaled with the measured lift force, than the extent of the porous material. To put it differently, porous airfoils with an air flow resistivity that is too low do not lead to a reduction of the buoyancy-corrected trailing edge noise at all, and the extent of the porous materials then of course has no impact. Additionally, the acoustic results, and especially the trailing edge noise spectra scaled with the lift force, show that it is necessary to perform further measurements on partially porous airfoils made of materials with medium air flow resistivities, having values somewhere between those of Porex and Recemat.

III.C. Boundary layer parameters

Hot-wire measurements were performed on the non-porous reference airfoil and three porous airfoils, with different extents of the porous material, at a flow speed U_0 of approximately 50 m/s ($Ma \approx 0.15$). Some additional measurements at a lower flow speed of approximately 34 m/s ($Ma \approx 0.10$) were performed on the non-porous airfoil and two of the three porous airfoils.

Figures 10 and 11 show both the mean velocity profiles and the turbulence intensity measured at the four airfoils. Regarding the air flow resistivity r of the porous materials, it can be concluded from Figure 10(a) and Figure 11(a) that a decreasing air flow resisitivity leads to an increasing thickness of the turbulent boundary layer and an increasing wake deficit. A decrease of the air flow resistivity of the porous materials also leads to an increase of the turbulence intensity both above the trailing edge and in the wake of the airfoils (Figures 10(b) and 11(b)). This is in accordance to the findings from the study on fully porous airfoils.[11,12] With increasing streamwise extent s of the porous material, the boundary layer thickness, the wake deficit and the turbulence intensity increase, too. This dependence was expected, since zero extent of the porous material ($s/c_l = 0$) should give results consistent to those obtained at the non-porous reference airfoil and a full extent ($s/c_l = 1$) leads to the results of the fully porous airfoils. Additionally, both a very

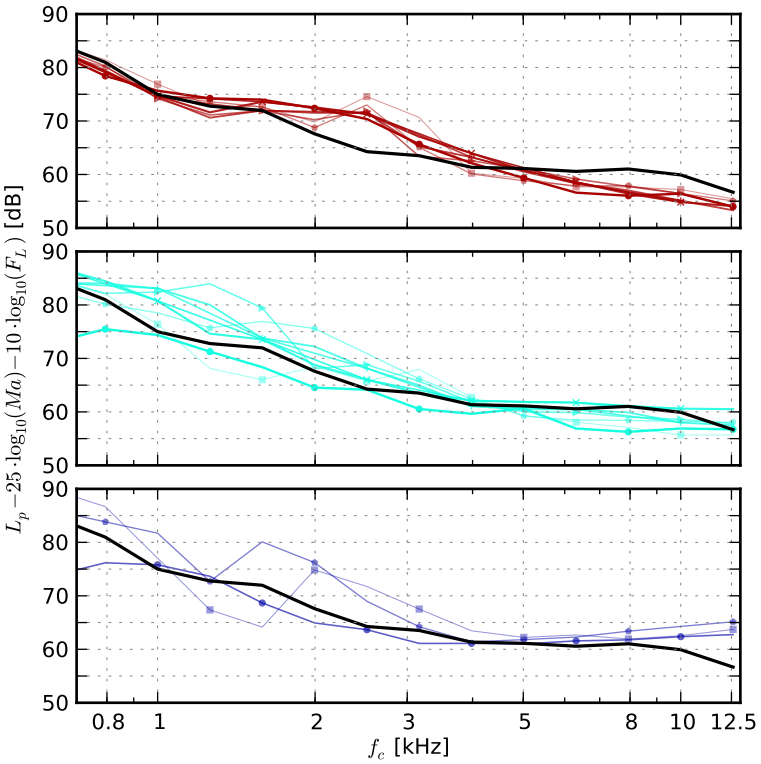

Figure 9. Trailing edge noise of selected airfoils at a flow speed of approximately 50 m/s, black: non-porous reference airfoil, $r = \infty$, colored: partly porous airfoils (materials: Porex, $r = 316{,}500$ Pa s/m^2, Recemat, $r = 8{,}200$ Pa s/m^2, M-Pore Al 45 ppi, $r = 1{,}000$ Pa s/m^2, extent: $s/c_l =$ ■ 0.05, ⬟ 0.1, ▶ 0.2, + 0.3, × 0.5, ● 1)

low air flow resistivity and a large extent of the porous material lead to a partial filling of the wake deficit, which is most likely caused by an internal flow inside the porous airfoil.

It has to be noted that not only the porosity of the porous trailing edges, but also the accompanying surface roughness affects the parameters of the turbulence within the boundary layer. For example, an increase in surface roughness will also lead to an increase of the turbulence intensity and an increase of the boundary layer thickness. A quantitative investigation of the influence of the surface roughness of the porous airfoils of the present study on the turbulence is still needed, but some additional aspects are discussed in reference.[12]

In order to gain a more general understanding of the processes that are responsible for the trailing edge noise reduction, third octave band spectra of the turbulent velocity fluctuations, measured in the turbulent boundary layer at a distance of 0.5 mm above the trailing edge (at $x/c_l = 1$) on the suction side of the airfoils are examined. The underlying assumption is that a manipulation of the turbulence spectrum within the boundary layer due to the porous consistency of the airfoils is responsible for the differences in the generated trailing edge noise. Furthermore, it is assumed that there is a relation between the spectral shape of the velocity fluctuations and the size of the pores, and thus to the air flow resistivity of the open porous materials.

Figure 12 and Figure 13 show the turbulence spectra measured above the trailing edge of the non-porous reference airfoil and three porous airfoils with varying extents of the porous material, again for two flow speeds. The results confirm the assumed cause of the narrow spectral peaks determined in the acoustic spectra in Figure 6 for the airfoils made of Recemat ($r = 8{,}200$ Pa s/m^2) and M-Pore Al 45 ppi ($r = 1{,}000$ Pa s/m^2) as these peaks are now also visible in the turbulence spectra, dependent on the extent s of the porous material. With increasing extent, the width of the peak increases and the peak shifts to lower frequencies. For the airfoil made of Porex ($r = 316{,}500$ Pa s/m^2), where a peak was found in the acoustic spectra at a constant Strouhal number, independent of the extent of the porous material, no clear peak is visible in the turbulence spectra. This is a further indicator that the acoustic peak may be a contribution of trailing edge thickness noise. An additional very small peak at a Strouhal number of approximately 1.1 is visible in the turbulence spectra of the airfoils (apart from those where this small peak is masked by the

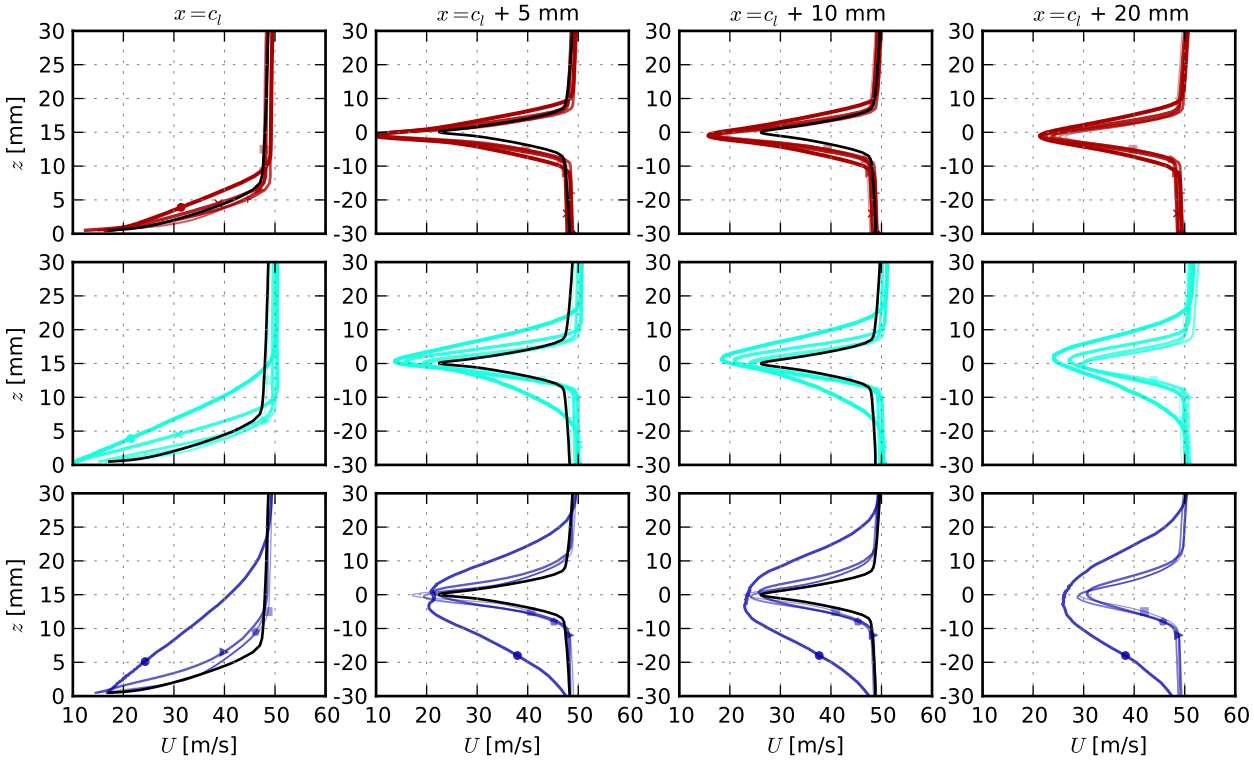

(a) Mean flow velocity U

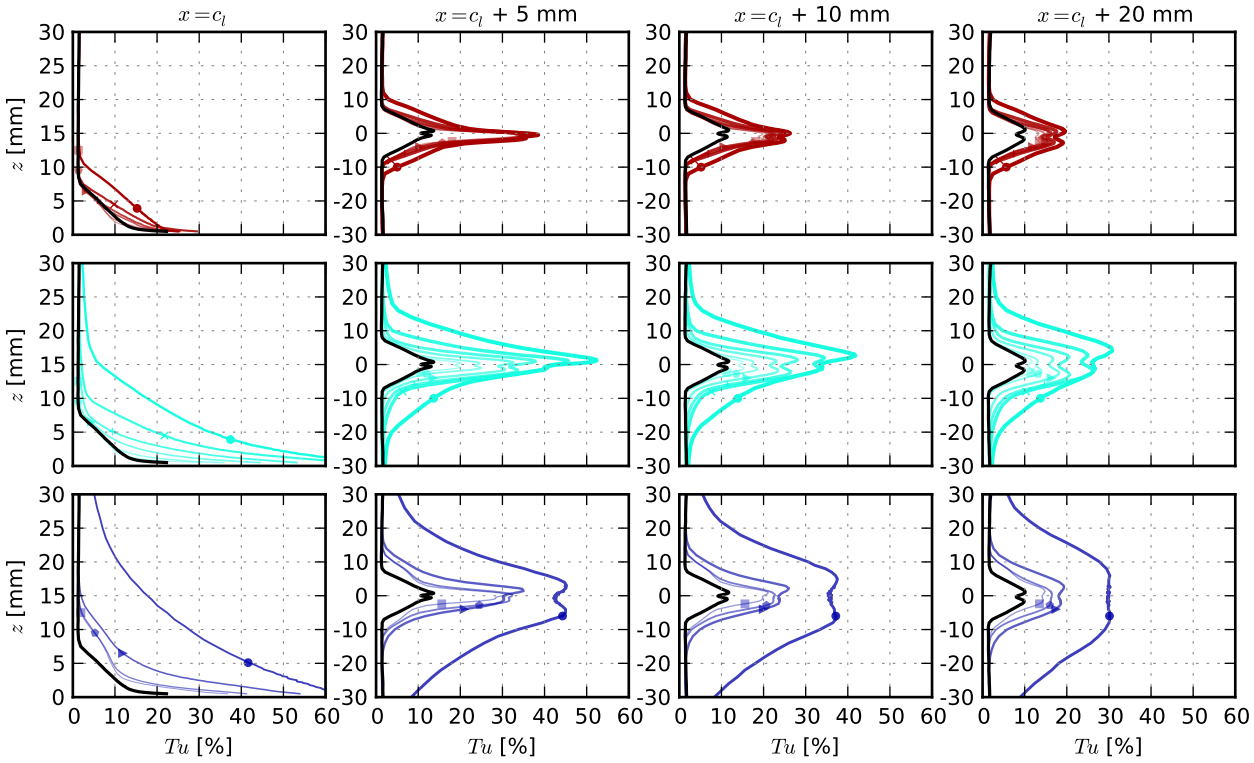

(b) Turbulence intensity $Tu = \sqrt{\overline{u^2}}/U$

Figure 10. Mean flow velocity and turbulence intensity measured above the trailing edge (first column) and in the wake (second, third and fourth column) of selected airfoils at a flow speed of approximately 50 m/s ($Ma \approx 0.15$), $r =$ ∞, 316,500 (Porex), 8,200 (Recemat) and 1,000 Pa s/m^2 (M-Pore Al), extent: $s/c_l =$ ■ 0.05, ⬟ 0.1, ▶ 0.2, + 0.3, × 0.5, ● 1

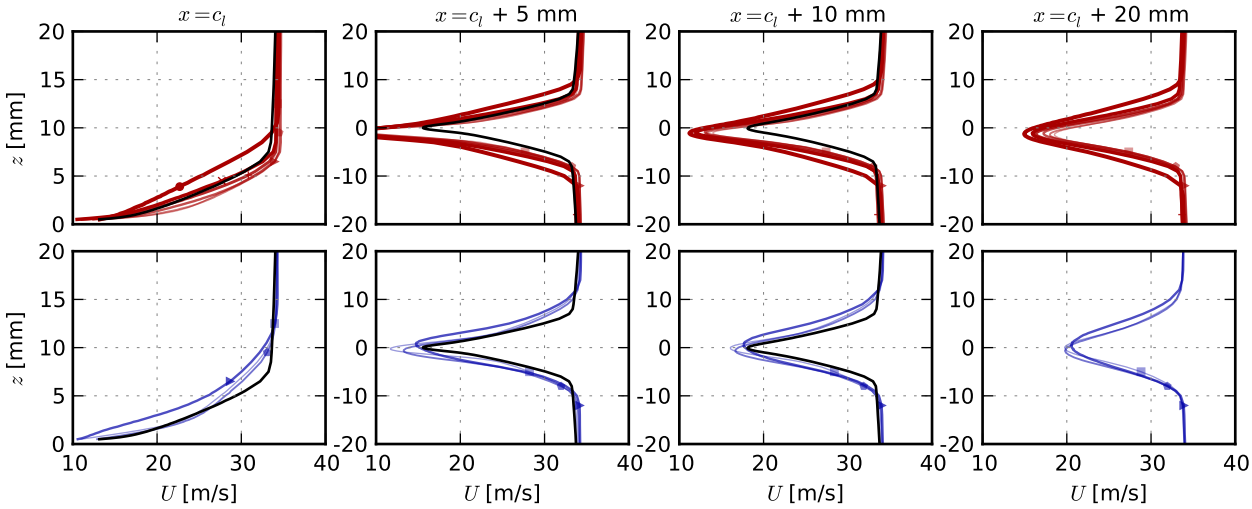

(a) Mean flow velocity U

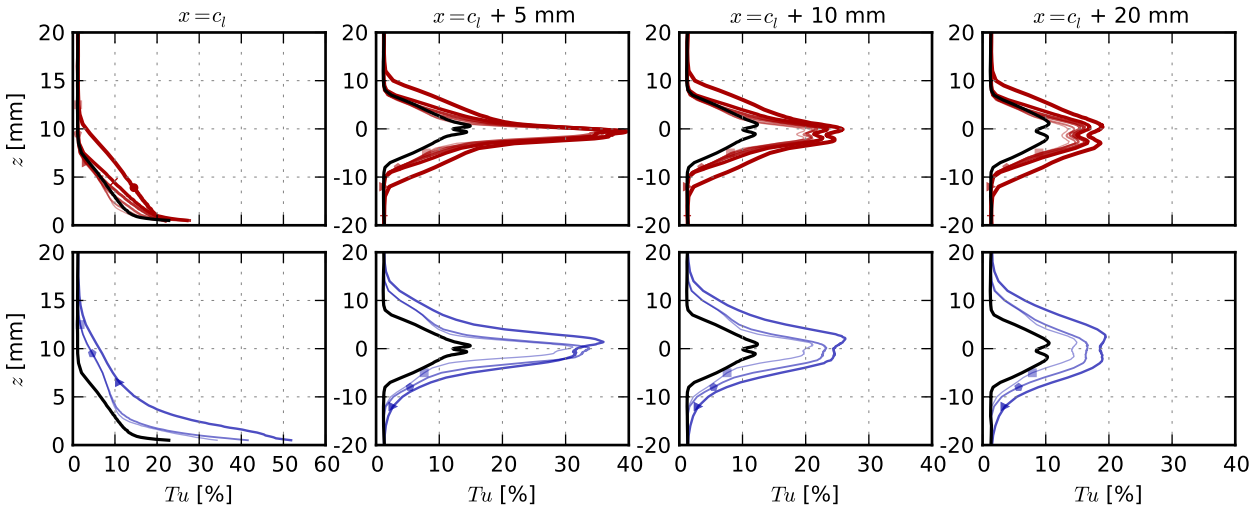

(b) Turbulence intensity Tu

Figure 11. Mean flow velocity and turbulence intensity measured above the trailing edge (first column) and in the wake (second, third and fourth column) of selected airfoils at a flow speed of approximately 34 m/s ($Ma \approx 0.10$), $r =$ ∞, 316,500 (Porex) and 1,000 Pa s/m^2 (M-Pore Al), extent: $s/c_l =$ ■ 0.05, ⬟ 0.1, ▶ 0.2, + 0.3, × 0.5, ● 1

strong peak). This peak is assumed to be related to other mechanisms, for example to velocity fluctuations that are already contained in the fluid flow. It is assumed to not be caused by the boundary layer flow over the surface of the airfoils. Apart from this peak, the turbulence spectrum of the non-porous reference airfoil shows no narrowband spectral characteristics.

The observation of the turbulence spectra in Figures 12 and 13 allows to draw conclusions on the cause of the noise reduction that is possible through the use of porous airfoils. It is visible that the amplitude of the turbulence spectra of the porous airfoils is below that of the reference airfoil only for high Strouhal numbers. This is roughly consistent to the Strouhal number range where an actual noise reduction was measured (Figs. 6 and 8). At very low Strouhal numbers, corresponding to the frequency range below the lower limit of the acoustic measurement setup, the amplitude of the turbulent velocity fluctuations of the porous airfoils exceeds that of the non-porous airfoil. Therefore, it has to be assumed that the use of porous airfoils does not lead to a noise reduction in this frequency range, but may even lead to a noticeable increase in trailing edge noise.

In accordance to the findings in reference[12] it is believed that the cause of the trailing edge noise reduction at high Strouhal numbers is the shift of the turbulence spectra towards lower frequencies when the turbulent structures move over the porous surface. In the present investigation this theory is supported by

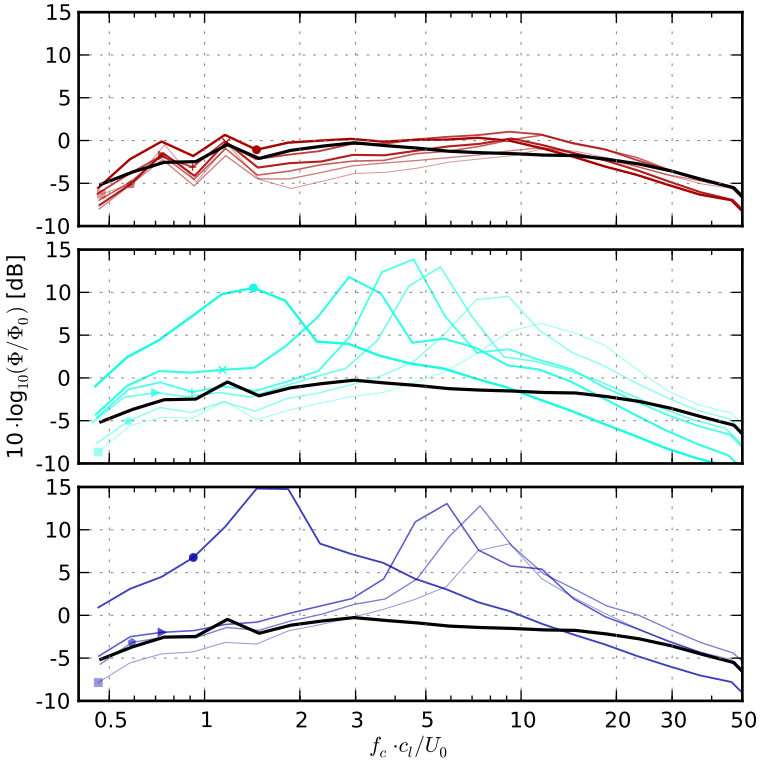

Figure 12. Third octave band spectra Φ of the turbulent velocity fluctuations, nondimensionalized by $\Phi_0 = 1$ m^{2}s^{-1}, measured at a flow speed of approximately 50 m/s ($Ma \approx 0.15$), $r =$ ∞, 316,500 (Porex), 8,200 (Recemat) and 1,000 Pa s/m^2 (M-Pore Al), extent: $s/c_l =$ ■ 0.05, ⬟ 0.1, ▶ 0.2, + 0.3, × 0.5, ● 1

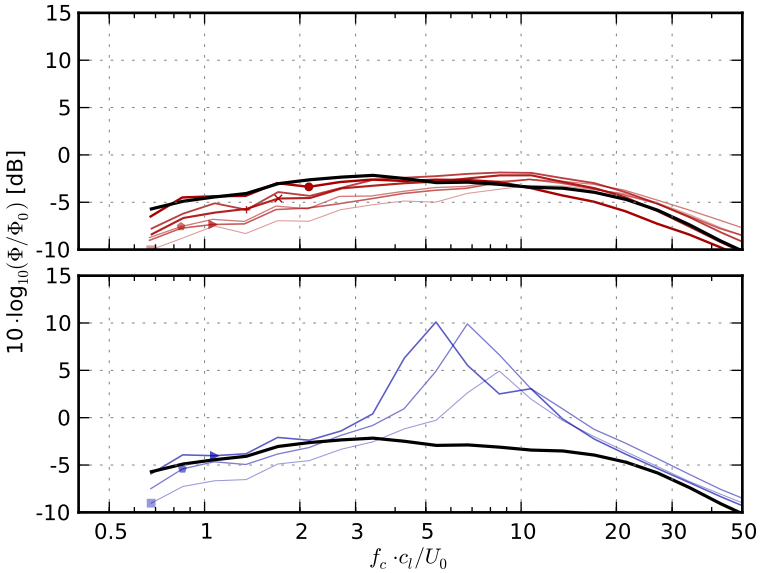

Figure 13. Third octave band spectra Φ of the turbulent velocity fluctuations, measured 0.5 mm above the trailing edge (at $x/c_l = 1$), nondimensionalized by $\Phi_0 = 1$ m^{2}s^{-1}, measured at a flow speed of approximately 34 m/s ($Ma \approx 0.10$), $r =$ ∞, 316,500 (Porex) and 1,000 Pa s/m^2 (M-Pore Al), extent: $s/c_l =$ ■ 0.05, ⬟ 0.1, ▶ 0.2, + 0.3, × 0.5, ● 1

the observation that for airfoils with a small streamwise extent s of the porous materials the spectral peak of the turbulent velocity fluctuations is at a higher frequency than for the same basic porous airfoil with a larger extent s, in which case the turbulent structures are simply convected over a larger part of the porous surface. Additionally, it is assumed that at high frequencies the corresponding small turbulent structures interact with the porous surface and their energy is dissipated into heat, an effect called hydrodynamic damping.

IV. Conclusions

In the present paper, a preliminary investigation of the trailing edge noise reduction of airfoils with varying extents of different porous materials (partially porous airfoils) compared to a non-porous reference airfoil is described in detail. These partially porous airfoils were obtained by simply covering a large part of the surface of fully porous airfoils from a previous study using a thin, impermeable foil. Acoustic measurements were conducted in an open jet wind tunnel using microphone array measurement technique and a three-dimensional deconvolution beamforming algorithm. In order to include the aerodynamic performance in the analysis of the measured trailing edge noise spectra, the lift force and drag force were measured simultaneously to the acoustic measurements. To allow for conclusions on the mechanisms that are responsible for the trailing edge noise reduction, constant temperature anemometry measurements were performed on selected airfoils.

The results of the acoustic measurements show that, without consideration of the aerodynamic performance of the porous airfoils, those airfoils with a larger extent of the porous material lead to a higher noise reduction compared to the non-porous reference airfoil. Regarding the properties of the open porous material the results suggest that materials with medium to high air flow resistivities lead to the maximum noise reduction at chord based Strouhal numbers approximately between 10 and 70. When scaled with the measured lift forces, as a simple approach to account for aerodynamic performance, it is visible that porous airfoils with low air flow resistivities are not feasible any more due to their poor aerodynamic performance. Porous airfoils with high air flow resistivities still lead to a noticeable reduction of trailing edge noise, even with only a small streamwise extent of the porous material.

The hot-wire measurements in the turbulent boundary layer and the wake of selected airfoils revealed that a decrease of the air flow resistivity of the porous airfoils leads to an increasing thickness of the boundary layer, an increasing wake deficit and an increasing turbulence intensity above the trailing edge and in the wake. An increasing streamwise extent of the porous materials also leads to an increase of the boundary layer thickness, the wake deficit and the turbulence intensity.

Additionally, third octave band spectra of the turbulent velocity fluctuations measured above the trailing edge of the airfoils were examined. For two of the porous airfoils, these turbulence spectra show strong spectral peaks that can also be found in the corresponding trailing edge noise spectra. It is assumed that the trailing edge noise reduction of the porous airfoils, which was measured at relatively high Strouhal numbers, is related to the lower turbulence energy in the corresponding frequency range. At frequencies below the frequency limit of the acoustic measurement setup, the turbulence energy of the porous airfoils exceeds that of the non-porous airfoil, leading to the assumption that the trailing edge noise is also higher in this frequency range. It is assumed that the trailing edge noise reduction at high Strouhal numbers is mainly caused by a shift of the turbulence spectra of the porous airfoils towards lower frequencies, combined with hydrodynamic damping at high frequencies.

Acknowledgements

The authors thank Manuel Bartsch and Falko Krüger for their help with the measurements. The financial support of the *Deutsche Forschungsgemeinschaft* in the priority program 1207, "Nature Inspired Fluid Mechanics", under the grant number SA 1502/1-3 is gratefully acknowledged.

References

[1]Amiet R K (1978) Refraction of Sound by a Shear Layer. J Sound Vib 58:467 - 482

[2]Bohn A J (1976) Edge noise attenuation by porous-edge extensions. AIAA 14th Aerospace Sciences Meeting, Seattle, WA, AIAA Paper 76-80

[3]Brooks T F, Marcolini M A, Pope D S (1986) Airfoil trailing-edge flow measurements. AIAA Journal 24

[4]Brooks T F, Humphreys W M (2006) A deconvolution approach for the mapping of acoustic sources (DAMAS) determined from phased microphone arrays. J Sound Vib 294:856 - 879

[5]Chanaud R C (1972) Noise reduction in propeller fans using porous blades at free-flow conditions. J Acoust Soc Am 51, 15 - 18

[6]Chanaud R C, Kong N, Sitterding R B (1976) Experiments on porous blades as a means of reducing fan noise. J Acoust Soc Am 59, 564 - 575

[7]Clennell M B (1997) Tortuosity: a guide through the maze. Geological Society, London, Special Publications 122:299-344

[8]Ffowcs Williams, J. E., Hall, L. H., Aerodynamic sound generation by turbulent flow in the vicinity of a scattering half plane, Journal of Fluid Mechanics, 40, 4, 657 - 670 (1970)

[9]Finez A, Jondeau E, Roger M, Jacob M C (2010) Broadband noise reduction with trailing edge brushes. 16th AIAA/CEAS Aeroacoustics Conference, Stockholm, Sweden, AIAA-paper 2010-3980

[10]Geyer T, Sarradj E, Fritzsche C (2010) Measurement of the noise generation at the trailing edge of porous airfoils. Exp Fluids 48:291 - 308

[11]Geyer T, Sarradj E, Fritzsche C (2010) Porous airfoils: noise reduction and boundary layer effects. Int J Aeroacoust 9(6):787 - 820

[12]Geyer T (2011) Trailing edge noise generation of porous airfoils. Dissertation, Brandenburg University of Technology Cottbus

[13]Geyer T, Sarradj E, Giesler J (2012) Application of a Beamforming Technique to the Measurement of Airfoil Leading Edge Noise. Adv Acoust Vib, Vol. 2012, Article ID 905461, doi:10.1155/2012/905461

[14]Gruber M, Joseph P F, Chong T P (2011) On the mechanisms of serrated airfoil trailing edge noise reduction. 17th AIAA/CEAS Aeroacoustics Conference, Portland, OR, AIAA-paper 2011-2781

[15]Herr M (2007) Design criteria for low-noise trailing edges. 13th AIAA/CEAS Aeroacoustics Conference, Rome, Italy, AIAA-paper 2007-3470

[16]Herr M, Reichenberger J (2011) In search of airworthy trailing-edge noise reduction means. 17th AIAA/CEAS Aeroacoustics Conference, Portland, OR, AIAA-paper 2011-2780

[17]ISO 9053 (1993) Acoustics – Materials for acoustical applications – Determination of airflow resistance. International Organization for Standardization

[18]Jaworski J, Peake N (2013) Aerodynamic noise from a poroelastic edge with implications for the silent flight of owls. J Fluid Mech, 723, 456-479

[19]Lasagna P L, Mackall K G, Burcham Jr. F W, Putnam T W (1980) Landing approach airframe noise measurements and analysis. NASA Technical Paper 1602

[20]Lilley G M (1998) A study of the silent flight of the owl. 4th AIAA/CEAS Aeroacoustics Conference, Toulouse, France, AIAA paper 98-2340

[21]Moreau D J, Brooks L A, Doolan C J (2012) On the noise reduction mechanism of a flat plate serrated trailing edge at low-to-moderate Reynolds number. 18th AIAA/CEAS Aeroacoustics Conference, Colorado Springs, CO, AIAA-paper 2012-2186

[22]Mueller T J (ed.) (2002) Aeroacoustic Measurements. Springer Science+Business Media, Berlin

[23]Oerlemans S, Migliore P (2004) Aeroacoustic wind tunnel tests of wind turbine airfoils. National Aerospace Laboratory Techreport NLR-TP-2004-319, The Netherlands (also presented at the 10th AIAA/CEAS Aeroacoustics Conference, Manchester, Great Britain, as AIAA-paper 2004-3042)

[24]Oerlemans S, Fisher M, Maeder T, Kögler K (2009) Reduction of wind turbine noise using optimized airfoils and trailing-edge serrations. AIAA J 47(6): 1470 - 1481

[25]Revell J D, Kuntz H L, Balena F, Horne W C, Storms B L, Dougherty R (1997) Trailing edge flap noise reduction by porous acoustic treatment, 3rd AIAA/CEAS Aeroacoustics Conference, Atlanta, GA, AIAA-paper 97-1646-CP

[26]Sarradj E, Fritzsche C, Geyer T, Giesler J (2009) Acoustic and Aerodynamic Design and Characterization of a Small-Scale Aeroacoustic Wind Tunnel, Appl Acoust, 70, 1073 - 1080

[27]Sarradj E (2010) A fast signal subspace approach for the determination of absolute levels from phased microphone array measurements. J Sound Vib 329:1553 - 1569

[28]Sarradj E (2012) Three-dimensional acoustic source mapping with different beamforming steering vector formulations. Adv Acoust Vib, Vol. 2012, Article ID 292695, doi:10.1155/2012/292695

[29]Sarradj E, Geyer T (2014) Symbolic regression modeling of noise generation at porous airfoils. Journal of Sound and Vibration (in press), doi: 10.1016/j.jsv.2014.02.037

[30]Sijtsma P (2007) CLEAN based on spatial source coherence. 13th AIAA/CEAS Aeroacoustics Conference, Rome, Italy, AIAA-paper 2007-3436